

Time Dependent Variational Principle with Ancillary Krylov Subspace

Mingru Yang* and Steven R. White

Department of Physics and Astronomy, University of California, Irvine, CA 92697, USA

(Dated: March 7, 2022)

We propose an improved scheme to do the time dependent variational principle (TDVP) in finite matrix product states (MPS) for two-dimensional systems or one-dimensional systems with long range interactions. We present a method to represent the time-evolving state in a MPS with its basis enriched by state-averaging with global Krylov vectors. We show that the projection error is significantly reduced so that precise time evolution can still be obtained even if a larger time step is used. Combined with the one-site TDVP, our approach provides a way to dynamically increase the bond dimension while still preserving the unitarity for the real time evolution. Our method is more accurate but has slower bond dimension growth than the conventional two-site TDVP.

Matrix product state (MPS) methods have obtained tremendous success in searching the ground state of one and two dimensional quantum lattice systems^{1–3}. There are also various developments in doing time evolution for finite^{4–8} and infinite^{9,10} systems to study the dynamical and finite-temperature properties.

Nevertheless, the current MPS methods for time evolution all have its own drawbacks. The original tDMRG⁴ and TEBD^{5,6} can only treat nearest-neighbor local interactions. For longer-range interactions, one can use swap gates to move the interacting sites to neighbor each other or use more center sites¹¹. But this variant fails for long-range interactions with long tails due to the large number of swap operations needed. In addition, the truncation in tDMRG and TEBD breaks the unitarity of the real time evolution. As an improvement of TEBD for matrix product density operators (MPDO)¹², the density matrix truncation (DMT)¹³ has been proposed to conserve the local observables. The matrix product operator (MPO) $W^{1,II}$ method⁷ approximate the MPO for the exponential of the Hamiltonian and thus able to treat long range interactions, but usually has a larger error in time-step and the more accurate second-order approximation unfortunately also breaks the unitarity of the real time evolution by using complex time steps.

TDVP¹⁰ is another method which can treat long-range interactions. The single-site TDVP has the advantages that its symplectic nature automatically preserves the integrals of motion for the real time evolution¹⁴. But the fixed finite bond dimension and single-site update might restrict the time evolution so that it deviates from the correct path¹⁵ because of the inadequate number of variational parameters. An example would be the initial state being a product state, which is the case for the minimally entangled typical thermal state (METTS)^{16,17} and the infinite temperature mixed state after purification¹⁸. The bond dimension of the MPS will be one and the projection error will be extremely large for the single-site TDVP. The two-site alternative⁸ of TDVP can encapsulate the entanglement growth by increasing the bond dimension dynamically but like the other methods the truncation again breaks the unitarity of the real-time evolution. In addition, for two-dimensional systems and systems with long-range interactions, even the two-site

TDVP can have large projection errors.

Since the single-site TDVP is efficient, able to embrace the long-range interactions, and respect the conservation laws¹⁹, it would be useful to relieve the issue of projection errors while retaining the advantages above so as to give rise to a more versatile method.

There have been some tricks to enlarge the bond dimension of the product state to be time evolved by the single-site TDVP. The original MPS can be embedded in a MPS with larger bond dimension by filling up zeros²⁰, but according to our tests, this approach fails to work¹⁴. Another way is to use several DMRG sweeps to introduce some noises which artificially increase the bond dimension²¹. But our test shows that for two-dimensional systems and long-range interactions, large errors emerge after a short time even though the bond dimension has been enlarged more than what is indeed necessary.

In fact increasing the bond dimension to a large value at the beginning and keeping it through the whole time evolution is not a reasonable choice, since the bond dimension needed for the initial time might be much smaller than the later time, and an unnecessary large bond dimension will slow down the calculation. It is suggested^{15,21} to first use two-site TDVP to increase the bond dimension for the initial sweeps and then switch to the single-site TDVP. However, the two-site TDVP breaks the unitarity of the real time evolution and if the initial state has a very small bond dimension we still face the issue of reducing the projection error for long range interactions, so we need to either enlarge the bond dimension before the time evolution or use an extremely small time step.

In this article, we propose a different to dynamically enlarge the bond dimension of the finite MPS to be time evolved by a follow-up single-site TDVP sweep, thereby reducing the projection errors by improving its tangent space even for large time steps and long-range interactions. Unlike in the exact diagonalization^{22,23}, in our algorithm the global Krylov vectors serve as ancillary MPS's to enrich the basis of the time evolving MPS through the gauge degree of freedom, thus avoiding the problems of loss of orthogonality and production of unnecessarily highly entangled state²¹.

I. ALGORITHMS

In this section, we will first introduce the MPS representation of a mixed state and then describe the global and local version of our new subspace expansion algorithms. We will also discuss the trick to preserve the unitarity for the real-time evolution.

A. Basis extension

As explained in Appendix A, the MPS representation of a physical state is not unique. We can utilize the gauge degree of freedom to extend the basis at each bond so as to get a MPS with enlarged bond dimension without changing the physical state.

Now suppose we have two MPS's $|\psi\rangle$ and $|\tilde{\psi}\rangle$ in their left canonical form as illustrated in FIG. 1,

$$\begin{aligned} |\psi\rangle &= \sum_{s_1 \dots s_N} A_1^{s_1} \dots A_{N-1}^{s_{N-1}} C_N^{s_N} |s_1 \dots s_N\rangle, \\ |\tilde{\psi}\rangle &= \sum_{s_1 \dots s_N} \tilde{A}_1^{s_1} \dots \tilde{A}_{N-1}^{s_{N-1}} \tilde{C}_N^{s_N} |s_1 \dots s_N\rangle, \end{aligned} \quad (1)$$

and we want to extend the bond basis of $|\psi\rangle$ by that of $|\tilde{\psi}\rangle$. A naive way to achieve that is to use the direct sum, i.e.

$$\begin{aligned} \begin{bmatrix} |\psi\rangle \\ |\tilde{\psi}\rangle \end{bmatrix} &= \sum_{s_1 \dots s_N} A_1^{s_1} \dots A_{N-1}^{s_{N-1}} C_N^{s_N} |s_1 \dots s_N\rangle \\ &= \sum_{s_1 \dots s_N} \begin{bmatrix} A_1^{s_1} & 0 \\ 0 & \tilde{A}_1^{s_1} \end{bmatrix} \dots \begin{bmatrix} A_{N-1}^{s_{N-1}} & 0 \\ 0 & \tilde{A}_{N-1}^{s_{N-1}} \end{bmatrix} \begin{bmatrix} C_N^{s_N} \\ \tilde{C}_N^{s_N} \end{bmatrix} |s_1 \dots s_N\rangle. \end{aligned} \quad (2)$$

In this way we get two states share a common MPS representation with an extra index in the first site that labels the two states. We can compress it to get a more economical representation by doing SVD from the right end to the left, which will end up with

$$\begin{bmatrix} |\psi\rangle \\ |\tilde{\psi}\rangle \end{bmatrix} = \sum_{s_1 \dots s_N} \begin{bmatrix} C_1^{s_1} \\ \tilde{C}_1^{s_1} \end{bmatrix} B_2^{s_2} \dots B_N^{s_N} |s_1 \dots s_N\rangle. \quad (3)$$

If we keep both $C_1^{s_1}$ and $\tilde{C}_1^{s_1}$, we will get a common MPS representation shared by $|\psi\rangle$ and $|\tilde{\psi}\rangle$, which can be used to do MPS summation $a|\psi\rangle + b|\tilde{\psi}\rangle$. If we throw $\tilde{C}_1^{s_1}$, we will get a right canonical MPS of $|\psi\rangle$ with its bond basis extended by $|\tilde{\psi}\rangle$ and an orthogonality center C_1 that does not have full column rank. The new MPS of $|\psi\rangle$ will have an enlarged bond dimension as long as not all the bond basis of $|\tilde{\psi}\rangle$ is linearly dependent on that of $|\psi\rangle$.

However, this naive approach has several drawbacks. First, it is not suitable for basis extension involving multiple MPS's. Suppose we have k MPS's now and want to use the latter $k-1$ MPS's to extend the basis of the first one, then the time complexity of SVD will be $O(k^3)$

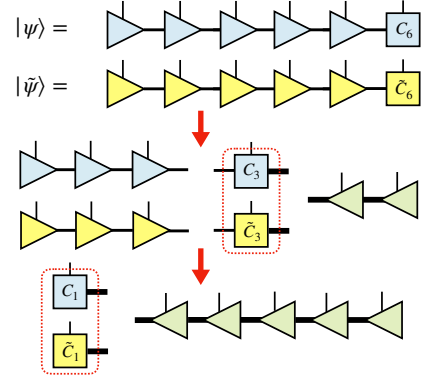


FIG. 1. Basis extension of $|\psi\rangle$ by $|\tilde{\psi}\rangle$.

larger if we use the direct sum. Second, the purpose can not be fulfilled if we only want to add part of the basis of $|\tilde{\psi}\rangle$ to $|\psi\rangle$. Finally, if we truncate in the SVD to make sure the bond dimension does not become too large, this way will not guarantee the information of the first MPS is not lost and for real time evolutions the unitarity will be broken since we truncate them all together.

Density matrices²⁴ are natural to solve the first problem. SVD the direct sum in Eq. 2 is equivalent to diagonalizing $\rho^R + \tilde{\rho}^R$, the sum of the reduced density matrix of the right partition of each state (see Appendix C for a proof). In this way we do not need to explicitly form the direct sum of site tensors, which is $O(k^2)$ times larger in size than the original site tensor of $|\psi\rangle$, but we only need to sum m reduced density matrices to get one of the same size and diagonalize it. Then the time complexity reduced to $O(k)$ times, similar to the tree-like way to do SVD.

We can solve the latter two problems by orthogonalizing the basis to be added into $|\psi\rangle$ against the existing basis and truncate them separately. Now we still take the case of two MPS's as an example. At site i , instead of directly SVD C_i' , we first SVD $C_i = U_i S_i V_i$ and form a projection operator $P_i = \mathbb{1} - V_i^\dagger V_i$ into the null space (the orthogonal complement of the row space) of $C_i : \mathcal{V} \rightarrow \mathcal{W}$,

$$\ker(C_i) = \{x \in \mathcal{V} \mid C_i x = 0\}, \quad (4)$$

where \mathcal{V} and \mathcal{W} is the column and row space respectively. Then we project \tilde{C}_i into C_i 's null space and SVD it, i.e.

$$\tilde{C}_i^\perp = \tilde{C}_i P_i = \tilde{U}_i^\perp \tilde{S}_i^\perp \tilde{V}_i^\perp. \quad (5)$$

We can truncate in this step of SVD to only keep $1 - \eta$ portion of the projected basis to add into $|\psi\rangle$. It is easy to prove $\tilde{V}_i^\perp V_i^\dagger = 0$ by $P_i^2 = P_i$, so we can enlarge the row space of V_i by the direct sum

$$V_i' = \begin{bmatrix} V_i \\ \tilde{V}_i^\perp \end{bmatrix}, \quad (6)$$

and get $U_i' S_i' = C_i' V_i'^\dagger$. We can continue doing that until reach the left end of the MPS. Similar procedure applies

to the density matrix formulation and $k > 2$ (see Appendix D).

It needs to be noticed that if $m_{i-1} \geq d_i m_i$, where m_{i-1} and m_i are the left and right bond dimension of C_i and d_i is the dimension of the local Hilbert space at site i , then $V_i^\dagger V_i = V_i V_i^\dagger = \mathbb{1}$ and $P_i = 0$, i.e. we will not add any new basis into $|\psi\rangle$ at site i .

B. Krylov subspace

How do we determine the states to be used to add basis into $|\psi\rangle$? A natural option is to use as $|\tilde{\psi}\rangle$ the polynomial approximation to the time evolved state

$$|\psi(t+\Delta t)\rangle = \exp(-i\hat{H}\Delta t)|\psi(t)\rangle \approx \sum_{l=0}^{k-1} \frac{(-i\Delta t)^l}{l!} \hat{H}^l |\psi(t)\rangle, \quad (7)$$

where $t + \Delta t$ can be either imaginary or real. Although the Taylor expansion usually converges slowly in k and we need a large k to get an accurate approximation to $|\psi(t+\Delta t)\rangle$, if we use it instead only as an ancillary MPS to extend the basis of $|\psi(t)\rangle$ before time evolution by a following TDVP sweep, the order k we need will be much smaller²⁵.

Actually the explicit MPS representation of $|\psi(t+\Delta t)\rangle$ is not needed to add basis into $|\psi(t)\rangle$. We only need the MPS's for each term $\hat{H}^l |\psi(t)\rangle$ in the Taylor expansion and use the $k-1$ MPS's to do basis extension as what we did in the last section. The states together span the k -dimensional Krylov subspace

$$\mathcal{K}_k(\hat{H}, |\psi\rangle) = \text{span}\{|\psi\rangle, \hat{H}|\psi\rangle, \dots, \hat{H}^{k-1}|\psi\rangle\}. \quad (8)$$

Usually the required k increases with the time step size.

There are three technical issues which need further elaboration. First, since the norm of $\hat{H}^l |\psi(t)\rangle$ grows exponentially with l , for numerical stability, we either normalize each MPS's or replace them by

$$(1 - i\tau\hat{H})|\psi(t)\rangle, \dots, (1 - i\tau\hat{H})^{k-1}|\psi(t)\rangle, \quad (9)$$

where τ is a small parameter to be tuned to make sure the norm of $\hat{H}^l |\psi(t)\rangle$ do not blow up. For imaginary time evolutions, we can choose $i\tau$ to be λ^{-1} , where λ is approximately the highest energy of the excited states. For real time evolutions, the choice of τ does not quite matter and we can simply set $\tau = \Delta t$. Those states still span the same Krylov subspace. Second, how do we apply \hat{H} efficiently? When the bond dimension of the MPO of \hat{H} is small, we can use the density matrix way²⁶ to apply it; otherwise we can use the variational way to apply it²¹. The complexity of apply \hat{H} at each site is comparable to one iteration of Lanczos to the integrate of the local effective equations B7 at site i in TDVP, but usually the number of iterations needed at a site in TDVP are much larger than k , so the time cost of the application of \hat{H} will be subleading.

The third issue is more tricky: how do we control the bond dimension of the MPS of $\hat{H}^l |\psi(t)\rangle$, which grows fast with increasing l if exact? Fortunately, for a reasonable choice of time step size, $k = 3$ can already get good accuracy, so the bond dimension growth from applying \hat{H} is not that problematic. On the other hand, we do not need to get an accurate $\hat{H}^l |\psi(t)\rangle$ so we can use a truncation error γ to control the number of new basis to be added by applying \hat{H} without affecting the norm of $|\psi(t)\rangle$. In addition, we can truncate $\eta = 10^{-8}$ or more when SVD \tilde{C}_i^\perp without affecting the accuracy, which controls the bond dimension of $|\psi(t)\rangle$ after basis extension. We can also truncate ϵ weights in the follow-up single-site TDVP for the imaginary time evolution. Furthermore, since the basis extension is conducted site by site, the implementation of the algorithm can be made less memory intensive by writing the unused parts of the MPS's to disk and reading them when need. The last thing to remember is that the basis extension is only needed to improve the tangent space at the initial stage of the time evolution, i.e. when the bond dimension of $|\psi(t)\rangle$ is not very large. As long as the bond dimension is large enough to get a good tangent space, our algorithm is not necessary anymore.

C. Subspace expansion

We call our basis extension algorithm the *global subspace expansion*^{27,28}. Combined with the single-site TDVP, the full improved scheme is as follows:

1. Construct the MPO $1 - i\tau\hat{H}$, and apply it to $|\psi(t)\rangle$ and get the set of MPS's in Eq. 9.
2. Do basis extension for $|\psi(t)\rangle$ as described in IA. (See Appendix E for a pseudo code of this step.)
3. Do the conventional single-site TDVP sweep.

As long as we use γ to control the bond dimension of the MPS after applying \hat{H} to be similar with or even smaller than $|\psi\rangle$, the complexity of step 1 is $O(4(k-1)m^3wd)$ if we apply it variationally²¹. The complexity in step 2 is $O((k-1)m^3d^2 + 3m^3d^3)$. The single-site TDVP has a complexity $O(2(k'-1)m^3w(d+1))$, where k' is the dimension of the local Krylov subspace. As described in the last section, usually $k' \gg k$ so the cost of step 1 and 2 will be comparable or less than step 3. In implementation, when we need to use this algorithm to extend the basis before a TDVP sweep can be determined by estimating the projection error¹⁴. Depending on the errors, we can use it once and do several succeeding TDVP sweeps before using it again.

The global algorithm is a little uneconomical since every time we use it before a TDVP sweep, we need to reconstruct the right edge tensors by contracting the right part of the MPO with the MPSs that sandwich it. To deal with it, similar to the idea of the subspace expansion for the single-site DMRG in²⁷, we propose a local way to

extend the basis for the single-site TDVP, i.e. at each local update of the conventional single-site TDVP we insert an extra step to enrich the basis. Since it only uses a different gauge condition, the derivation of the tangent space projector will remain the same. However, according to our tests, the required k and $1 - \eta$ of the *local subspace expansion* will be much larger than the *global* version to get a similar accuracy, which facilitates the bond dimension growth and thus slows down the calculation, so we do not recommend it. For more details one can go to Appendix F.

II. BENCHMARKS

A. Imaginary time evolution

To test the performance of our algorithms for imaginary time evolutions, we take as a first example a Heisenberg ladder of length 100 with its two legs weakly coupled from each other. To demonstrate the power of our methods, we let the weak inter-chain coupling go to zero so only next-nearest neighbor interactions remain after the zig-zag mapping to the MPS from the ladder geometry, which is a case that the conventional single-site TDVP (TDVP1) and two-site TDVP (TDVP2) completely fail if started from a product state of the ladder¹¹.

The Hamiltonian reads

$$\hat{H} = \sum_{r, \langle i, j \rangle} \hat{\mathbf{S}}_{r,i} \cdot \hat{\mathbf{S}}_{r,j}, \quad (10)$$

where $r \in \{1, 2\}$ denotes the rung index and $\langle i, j \rangle$ denotes the nearest-neighbor sites among each rung.

We perform an imaginary time evolution started from a Neel state $|\psi(0)\rangle$ and measure the energy $E = \langle \psi(t) | \hat{H} | \psi(t) \rangle$. When $t \rightarrow \infty$, $|\psi(t)\rangle = e^{-t\hat{H}} |\psi(0)\rangle$ should go to the ground state. We use $\gamma = 10^{-12}$ when applying $1 - i\tau\hat{H}$. We find that $i\tau = 1/40$, $k = 3$, and $\eta = 10^{-8}$ turns out to be the optimal parameter settings in this case for our method (GSE-TDVP1). Higher order k or smaller truncation η in the subspace expansion does not improve the accuracy. The results are shown in FIG. 2. We also put a comparison with the second-order MPO $W^{1,II}$ method and TDVP2. While TDVP2 fails as expected, GSE-TDVP1 has an accuracy 10^3 better than the MPO $W^{1,II}$, despite a faster bond dimension growth. However, that is because we do not truncate in the follow-up TDVP sweep, otherwise our method is able to get a slower bond dimension increase while still retaining a better energy accuracy, as shown in FIG. 2. We also try larger a time step $\Delta t = 0.4$, and get 10^{-3} accuracies using the same τ , k , and η , but meanwhile also get a faster bond dimension growth than $\Delta t = 0.1$. Again, it can be fixed by using a post-truncation ϵ in the follow-up TDVP1 sweep.

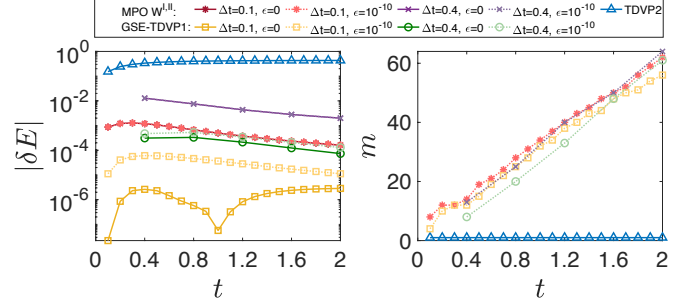


FIG. 2. Benchmark results of the imaginary time evolution for the rung-decoupled Heisenberg ladder. (Left) relative energy errors $\delta E = (E - E_0)/E_0$, where reference energy E_0 is got by doubling the energy obtained from TDVP2 with $\Delta t = 0.01$ for a single chain, which is supposed to be very accurate. (Right) Bond dimension m growth. We make the error in MPO $W^{1,II}$ second order by using complex time steps, and ϵ is the truncation error in applying $\exp(-\Delta t \hat{H})$. For GSE-TDVP1, we use the optimal setting $i\tau = 1/40$, $k = 3$, $\eta = 10^{-8}$, and ϵ is the truncation error in the follow-up TDVP1 sweep.

B. Real time evolution

We choose the one-axis twisted (OAT) model^{29,30} of a chain of length $N = 100$ as a benchmark for the real time evolution. Its Hamiltonian reads

$$\hat{H} = \chi(\hat{S}^z)^2, \quad (11)$$

where $\hat{S}^z = \sum_i \hat{S}_i^z$ and χ sets the timescale for the spin squeezing dynamics and can be absorbed into t . The interactions are all-to-all and infinitely long-ranged but its MPO representation is rather simple and only has a bond dimension $w = 3$. A initial state with all spins polarized in the $+x$ direction, i.e. $|\psi(0)\rangle = |\rightarrow\rangle^{\otimes N}$, will be quenched by H at $t = 0$, and this nonlinear interaction will squeeze the spins.

One can easily get $\langle \hat{S}^y(t) \rangle = \langle \hat{S}^z(t) \rangle = 0$ from $[\hat{H}, \hat{P}_x] = 0$, where \hat{P}_x is the reflection operator about the $y - z$ plane. One can also prove

$$\langle \hat{S}^x(t) \rangle = \frac{N}{2} \cos^{N-1}(\chi t). \quad (12)$$

Correlation functions are important to calculate the spin squeezing parameters $\xi^2(t)$, which is defined as

$$\xi^2 = N \min_{\mathbf{n}_\perp} \frac{\langle (\hat{\mathbf{S}} \cdot \mathbf{n}_\perp)^2 \rangle - \langle \hat{\mathbf{S}} \cdot \mathbf{n}_\perp \rangle^2}{\langle \hat{\mathbf{S}} \rangle^2}, \quad (13)$$

where $\hat{S}^\mu = \sum_i \hat{S}_i^\mu$ and \mathbf{n}_\perp is a unit vector perpendicular to $\langle \hat{\mathbf{S}} \rangle$. For the initial state being the $+x$ polarized state, $\langle \hat{\mathbf{S}} \rangle = \langle \hat{S}^x \rangle \mathbf{n}_x$, and to get ξ^2 we need $\langle \hat{S}^y \hat{S}^y \rangle$, $\langle \hat{S}^z \hat{S}^y \rangle$, $\langle \hat{S}^z \hat{S}^z \rangle$, where the last one is proportional to \hat{H} and thus should be conserved. Plug in their expressions and we can get the optimal spin squeezing ξ_{opt}^2

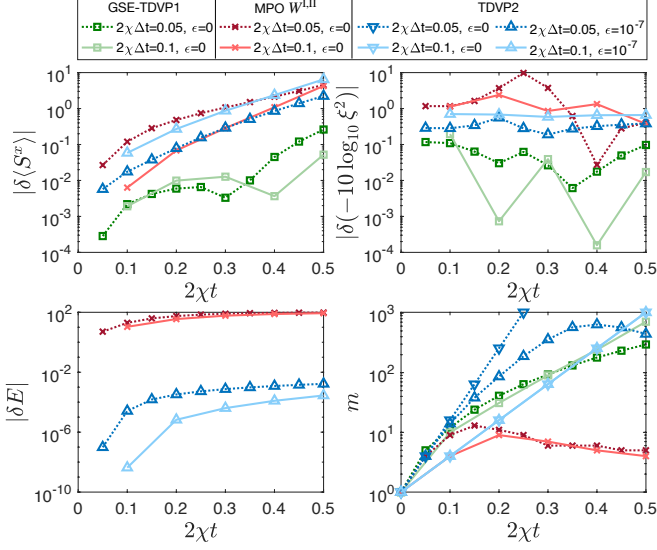


FIG. 3. Benchmark results of the real time evolution for the OAT model. $|\delta \cdot|$ is the absolute relative error of the corresponding quantity, where the reference value is from the analytical formula. For GSE-TDVP1, we use $\tau = \Delta t$, $k = 3$, $\gamma = 10^{-4}$, $\eta = 10^{-4}$ for $2\chi\Delta t = 0.05$, and $\tau = \Delta t$, $k = 5$, $\gamma = 10^{-4}$, $\eta = 10^{-8}$ for $2\chi\Delta t = 0.1$. We make the error in MPO $W^{I,II}$ second order by using complex time steps. ϵ in TDVP2 is the truncation error of SVD during the sweep. For TDVP2, the data points of $|\delta\langle S^x \rangle|$ and $|\delta(-10 \log_{10} 0 \xi^2)|$ for $\epsilon = 0$ are on top of $\epsilon = 0$ so we only show one of them. We do not show the curves of $|\delta E|$ for GSE-TDVP1 and TDVP2 at $\epsilon = 0$ since they are conserved up to the machine accuracy.

is expected to appear at $t_{\text{opt}} = 12^{\frac{1}{6}}(N/2)^{-\frac{2}{3}}/(2\chi)$. The entanglement will grow fast after t_{opt} , when various decoherent processes are involved.

In FIG. 3, we compare our method with TDVP2 and MPO $W^{I,II}$. To preserve the exact unitarity, we set $\epsilon = 0$ for our GSE-TDVP1 method. We tune γ and η instead to control the number of new basis added in, thus preventing the bond dimension of $|\psi(t)\rangle$ from becoming too large. Using $\tau = \Delta t$, $k = 3$, $\gamma = 10^{-4}$, $\eta = 10^{-4}$ for $2\chi\Delta t = 0.05$ and $\tau = \Delta t$, $k = 5$, $\gamma = 10^{-4}$, $\eta = 10^{-8}$ for $2\chi\Delta t = 0.1$ turn out to have the optimal balance between the cost and accuracy. Our method, being the most accurate again, also has slower bond dimension growth than the TDVP2, while preserving the unitarity exactly. We can see that for MPO $W^{I,II}$ the conservation of energy is terrible and the overall shape of ξ^2 is wrong. Actually, the MPO $W^{I,II}$ behaves extremely bad in this case because the all-to-all interaction will make the error in the approximation of the operator $\exp(-i\Delta t \hat{H})$ extremely large, and reducing the time step size to $2\chi\Delta t = 0.01$ would not even help.

III. CONCLUSIONS

In this paper, we present an efficient algorithm that can produce unprecedented accuracy for time evolution with long range interactions combined with the single-site TDVP. It provides a controllable way to improve the accuracy while using a larger time step and to dynamically enlarge the bond dimension for the single-site TDVP, thus solving the problem of the initial state being a product state. Our method enables people to perform reliable simulations of out-of-equilibrium dynamics and finite temperature properties in systems with long-range interactions and two dimensional systems.

Appendix A: Notations

A many-body state with open boundary conditions for a lattice of N number of sites with the local physical degrees of freedom labeled by s_n is given by

$$|\psi\rangle = \sum_{s_1 \dots s_N} c_{s_1 \dots s_N} |s_1 \dots s_N\rangle, \quad (\text{A1})$$

which can be decomposed as an finite MPS as

$$|\psi[M]\rangle = \sum_{s_1 \dots s_N} M_1^{s_1} \dots M_N^{s_N} |s_1 \dots s_N\rangle, \quad (\text{A2})$$

where M_n ($\forall n \in \{1, \dots, N\}$) are rank-3 tensors. An entry of it can be written as $[M_n]_{b_{n-1} b_n}^{s_n}$, where s_n is the physical index of dimension d_n and b_{n-1} and b_n are the left and right virtual indices of dimension m_{n-1} and m_n respectively. Usually $d_n \equiv d$ but m_n varies with n . For finite MPS, $m_0 = m_{N+1} = 1$ and $\max\{m_n\}$ is reached in the middle of the lattice. m_n is conventionally called the bond dimension for the n th bond of the lattice.

There is also a similar MPO representation of the Hamiltonian

$$\hat{H} = \sum_{s_1 \dots s_N, s'_1 \dots s'_N} W_1^{s_1 s'_1} \dots W_N^{s_N s'_N} |s_1 \dots s_N\rangle \langle s'_1 \dots s'_N|. \quad (\text{A3})$$

The MPS representation has redundancies called gauge freedom, i.e. the physical state $|\psi\rangle$ is invariant under the gauge transformation

$$M_n^{s_n} \mapsto M_n'^{s_n} = G_n^L M_n^{s_n} G_n^R, \quad (\text{A4})$$

where $G_{n-1}^R G_n^L = \mathbb{1}$ and $G_1^L = G_N^R = \mathbb{1}$. We can bring the MPS to canonical forms by fixing the gauge. For example, to get the mixed canonical form with the orthogonality center at site i

$$|\psi\rangle = \sum_{s_1 \dots s_N} A_1^{s_1} \dots A_{i-1}^{s_{i-1}} C_i^{s_i} B_{i+1}^{s_{i+1}} \dots B_N^{s_N} |s_1 \dots s_N\rangle, \quad (\text{A5})$$

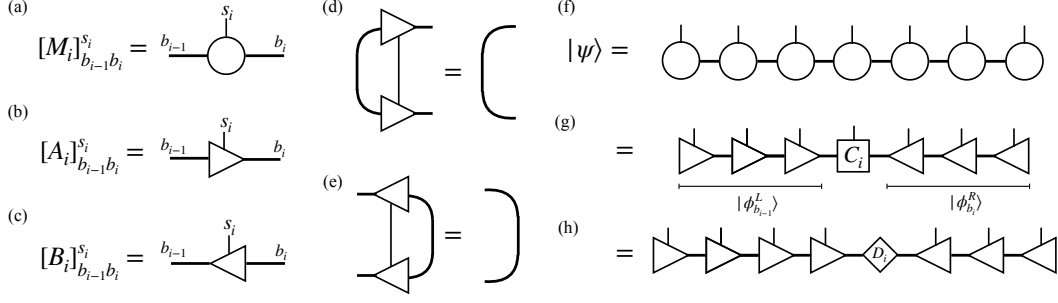


FIG. 4. Graphic notations.

where $A_n^{s_n}$ is left-orthonormal and $B_n^{s_n}$ is right-orthonormal, i.e.

$$\begin{aligned} \sum_{s_n} (A_n^\dagger)^{s_n} A_n^{s_n} &= \mathbb{1}, \\ \sum_{s_n} B_n^{s_n} (B_n^\dagger)^{s_n} &= \mathbb{1}, \end{aligned} \quad (\text{A6})$$

we can fix the gauge by the singular value decomposition (SVD) of the site tensors first from $n = 1$ to $n = N$ iteratively, i.e.

$$A_n^{s_n} G_{n+1}^L = U_n S_n V_n = G_n^L M_n^{s_n}, \quad (\text{A7})$$

where $G_n^L = S_{n-1} V_{n-1}$ to get the left-canonical form, and then SVD from $n = N$ to $n = 1$ iteratively, i.e.

$$G_{n-1}^R B_n^{s_n} = U_n S_n V_n = A_n^{s_n} G_n^R, \quad (\text{A8})$$

where $G_n^R = U_{n+1} S_{n+1}$ and we have

$$C_i^{s_i} = A_i^{s_i} D_i = D_{i-1} B_i^{s_i}, \quad (\text{A9})$$

where $D_i = U_{i+1} S_{i+1}$. Eq (A5) can also be rewritten as

$$|\psi\rangle = \sum_{b_{i-1} s_i b_i} [C_i]_{b_{i-1} b_i}^{s_i} |\phi_{b_{i-1}}^L\rangle |s_i\rangle |\phi_{b_i}^R\rangle, \quad (\text{A10})$$

where

$$|\phi_{b_{i-1}}^L\rangle = \sum_{s_1 \dots s_{i-1}} (A_1^{s_1} \dots A_{i-1}^{s_{i-1}})_{b_{i-1}} |s_1 \dots s_{i-1}\rangle \quad (\text{A11})$$

and

$$|\phi_{b_i}^R\rangle = \sum_{s_{i+1} \dots s_N} (B_{i+1}^{s_{i+1}} \dots B_N^{s_N})_{b_i} |s_{i+1} \dots s_N\rangle \quad (\text{A12})$$

are automatically orthonormal bases for the left and right partition of the lattice respectively.

We can define effective Hamiltonians through the canonical forms (as shown in FIG. 5). The single-site effective Hamiltonian $H(i)$ can be written as

$$[H(i)]_{b'_{i-1} s'_i b'_i; b_{i-1} s_i b_i} = \langle \phi_{b'_{i-1}}^R | \langle s'_i | \langle \phi_{b'_i}^L | \hat{H} | \phi_{b_{i-1}}^L \rangle | s_i \rangle | \phi_{b_i}^R \rangle. \quad (\text{A13})$$

Similarly using Eq (A9) we can rewrite

$$|\psi\rangle = \sum_{a_i b_i} [D_i]_{a_i b_i} |\phi_{a_i}^L\rangle |\phi_{b_i}^R\rangle, \quad (\text{A14})$$

and get the zero-site effective Hamiltonian $K(i)$

$$[K(i)]_{a'_i b'_i; a_i b_i} = \langle \phi_{b'_i}^R | \langle \phi_{a'_i}^L | \hat{H} | \phi_{a_i}^L \rangle | \phi_{b_i}^R \rangle. \quad (\text{A15})$$

Appendix B: The conventional TDVP

The TDVP⁸ corresponds to project the time-dependent Schrödinger equation to the tangent space of the MPS manifold \mathcal{M}_{MPS} at the current time t , i.e.

$$i \frac{d}{dt} |\psi[M]\rangle = \hat{P}_{T_{|\psi[M]\rangle} \mathcal{M}_{\text{MPS}}} \hat{H} |\psi[M]\rangle. \quad (\text{B1})$$

The one-site tangent space projector can be decomposed as

$$\hat{P}_{T_{|\psi[M]\rangle} \mathcal{M}_{\text{MPS}}} = \sum_{n=1}^N \hat{P}_{n-1}^L \otimes \hat{\mathbb{1}}_n \otimes \hat{P}_{n+1}^R - \sum_{n=1}^{N-1} \hat{P}_n^L \otimes \hat{P}_{n+1}^R, \quad (\text{B2})$$

where

$$\begin{aligned} \hat{P}_n^L &= \sum_{b_n=1}^{m_n} |\phi_{b_n}^L\rangle \langle \phi_{b_n}^L|, \\ \hat{P}_n^R &= \sum_{b_{n-1}=1}^{m_{n-1}} |\phi_{b_{n-1}}^R\rangle \langle \phi_{b_{n-1}}^R|. \end{aligned} \quad (\text{B3})$$

With the tangent space projector, the right hand side of Eq (B1) becomes

$$\begin{aligned} \hat{P}_{T_{|\psi[M]\rangle} \mathcal{M}_{\text{MPS}}} \hat{H} |\psi[M]\rangle &= \sum_{n=1}^N \sum_{b'_{n-1} s'_n b'_n; b_{n-1} s_n b_n} |\phi_{b'_{n-1}}^L\rangle \langle s'_n | \langle \phi_{b'_n}^R | [H(n)]_{b'_{n-1} s'_n b'_n; b_{n-1} s_n b_n} [C_n]_{b_{n-1} b_n}^{s_n} \\ &\quad - \sum_{n=1}^{N-1} \sum_{a'_n b'_n; a_n b_n} |\phi_{a'_n}^L\rangle \langle \phi_{b'_n}^R | [K(n)]_{a'_n b'_n; a_n b_n} [D_n]_{a_n b_n}. \end{aligned} \quad (\text{B4})$$

Actually Eq (B1) can be integrated into the form

$$|\psi(t + \Delta t)\rangle = \exp[-i\hat{P}_{T_{|\psi[M]\rangle}, \mathcal{M}_{\text{MPS}}} \hat{H} \Delta t] |\psi(t)\rangle. \quad (\text{B5})$$

The exponential operator in the right hand side can be splitted by the Lie-Trotter decomposition. To first order, it formally becomes

$$\begin{aligned} \exp[-i\hat{P}_{T_{|\psi[M]\rangle}, \mathcal{M}_{\text{MPS}}} \hat{H} \Delta t] &= \exp \\ &\left[-i \sum_{n=1}^N \hat{P}_{n-1}^L \otimes \hat{\mathbb{1}}_n \otimes \hat{P}_{n+1}^R \hat{H} \Delta t + i \sum_{n=1}^{N-1} \hat{P}_n^L \otimes \hat{P}_{n+1}^R \hat{H} \Delta t \right] \\ &= \exp[-i\hat{P}_{N-1}^L \otimes \hat{\mathbb{1}}_N \hat{H} \Delta t] \exp[i\hat{P}_{N-1}^L \otimes \hat{P}_N^R \hat{H} \Delta t] \\ &\quad \exp[-i\hat{P}_{N-2}^L \otimes \hat{\mathbb{1}}_{N-1} \otimes \hat{P}_N^R \hat{H} \Delta t] \dots \\ &\quad \exp[i\hat{P}_1^L \otimes \hat{P}_2^R \hat{H} \Delta t] \exp[-i\hat{\mathbb{1}}_1 \otimes \hat{P}_2^R \hat{H} \Delta t] \\ &\quad + \mathcal{O}(\Delta t^2). \quad (\text{B6}) \end{aligned}$$

Higher order decomposition can be derived accordingly. The decomposition above enables us to integrate the differential equation iteratively, i.e. at step n we assume only C_n is time-dependent so we only need to solve the local effective equations

$$\begin{aligned} i \frac{d}{dt} C_n(t) &= H(n) C_n(t), \\ -i \frac{d}{dt} D_n(t) &= K(n) D_n(t). \end{aligned} \quad (\text{B7})$$

Besides the Trotter error, there are errors from the projection to the tangent space, i.e.

$$\|(\hat{\mathbb{1}} - \hat{P}_{T_{|\psi[M]\rangle}, \mathcal{M}_{\text{MPS}}}) \hat{H} |\psi[M]\rangle\|. \quad (\text{B8})$$

The projection error can be estimated according to section III. F of¹⁴ and³¹. The key observation is that both the projection error and the Trotter error depend on the tangent space projector. Consider the limit that the states of which the projector consists form a complete basis. Then the projector is simply an identity operator. Consequently Eq (B8) becomes zero and each term in the Lie-Trotter splitting commutes with each other so the Trotter error also becomes zero. In other words, $\hat{H} |\psi[M]\rangle$ is still in the same manifold \mathcal{M}_{MPS} so the projection does not take any effect and the equation becomes the exact Schrödinger equation and the left hand side can be exactly equal to the right hand side of B1. However, exactly complete basis is not reachable when the system size becomes large and we always need to compress the MPS to have a finite bond dimension. To reduce the errors, the key is to get an approximate projector of certain bond dimension as close to the identity as possible. Since $\hat{P}_{T_{|\psi[M]\rangle}, \mathcal{M}_{\text{MPS}}}$ originates from the variational ansatz itself, the problem becomes how to obtain a good enough basis set for the variational ansatz. Although the physical variational ansatz is always the time-evolving state which is unchangeable, the MPS representation of it can indeed be varied through the gauge freedom. For example, the MPS representation of a product state do not

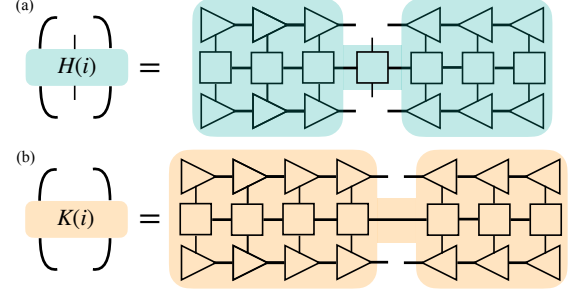


FIG. 5. The single-site and zero-site effective Hamiltonians.

necessarily have bond dimension to be one but can have the maximum bond dimension allowed at each bond with the orthogonality center being rank one, and therefore we can have complete bases for \hat{P}^L and \hat{P}^R even for a product state. If we re-orthogonalize the MPS, the bond dimension will shrink back to one, but if a time evolution is immediately followed at the orthogonality center, the bond dimension can be maintained.

Appendix C: Proof

In the following we prove that SVD C'_i in Eq. 2 is equivalent to diagonalizing the sum of the right reduced density matrix $\rho_i + \tilde{\rho}_i$.

At site N , if $C'_N = U'_N S'_N V'_N$, then

$$\begin{aligned} \rho'_N &= C'_N{}^\dagger C'_N = \left[C_N^\dagger \tilde{C}_N^\dagger \right] \begin{bmatrix} C_N \\ \tilde{C}_N \end{bmatrix} \\ &= C_N^\dagger C_N + \tilde{C}_N^\dagger \tilde{C}_N = \rho_N + \tilde{\rho}_N \\ &= V'_N{}^\dagger S'_N{}^2 V'_N. \end{aligned} \quad (\text{C1})$$

So at site N , we get the same V'_N in diagonalization of $\rho_N + \tilde{\rho}_N$ as in SVD of C'_N . We can write U'_N into a block form

$$U'_N = \begin{bmatrix} U_N \\ \tilde{U}_N \end{bmatrix} \quad (\text{C2})$$

so $C_N = U_N S'_N V'_N$ and $\tilde{C}_N = \tilde{U}_N S'_N V'_N$. Absorbing $U'_N S'_N$ into A'_{N-1} is equivalent to moving the orthogonality center to site $N-1$ separately for $|\psi\rangle$ and $|\tilde{\psi}\rangle$, i.e.

$$\begin{aligned} C'_{N-1} &= A'_{N-1} U'_N S'_N \\ &= \begin{bmatrix} A_{N-1} & 0 \\ 0 & \tilde{A}_{N-1} \end{bmatrix} \begin{bmatrix} U_N \\ \tilde{U}_N \end{bmatrix} S'_N \\ &= \begin{bmatrix} A_{N-1} U_N S'_N \\ \tilde{A}_{N-1} \tilde{U}_N S'_N \end{bmatrix} = \begin{bmatrix} A_{N-1} C_N V'_N{}^\dagger \\ \tilde{A}_{N-1} \tilde{C}_N V'_N{}^\dagger \end{bmatrix} \\ &= \begin{bmatrix} C_{N-1} \\ \tilde{C}_{N-1} \end{bmatrix}. \end{aligned} \quad (\text{C3})$$

Similar to C1, SVD C'_{N-1} is equivalent to diagonalizing $\rho_{N-1} + \tilde{\rho}_{N-1}$ and so on for all other sites. This proof can be extended to the cases of $k > 2$ MPS's.

Appendix D: Density matrix formulation when $k > 2$

In the following we show how to do basis extension with orthogonalization at site i .

After SVD $C_i = U_i S_i V_i$ and forming the projector P_i onto its null space, we first sum the reduced density matrices of the latter $k - 1$ MPS's, i.e.

$$\tilde{\rho}_i = \sum_{l=1}^{k-1} \rho_{l,i}, \quad (\text{D1})$$

where l labels the latter $k - 1$ MPS's. Then we project it into the null space of C_i

$$\tilde{\rho}_i^\perp = P_i \tilde{\rho}_i P_i, \quad (\text{D2})$$

which is equivalent to projecting each $\tilde{C}_{l,i}$ by P_i and direct summing them. Then we diagonalize and truncate it, resulting in $\tilde{\rho}_i^\perp = \tilde{V}_i^{\perp\dagger} \tilde{S}_i^{\perp 2} \tilde{V}_i^\perp$. Finally we enlarge the row space by the direct sum

$$V_i' = \begin{bmatrix} V_i \\ \tilde{V}_i^\perp \end{bmatrix}. \quad (\text{D3})$$

Appendix E: Global subspace expansion

In the following we summarize the step 2 of the global subspace expansion. It deals with how to extend the basis of the left canonical MPS of $|\psi\rangle$ by the left canonical MPS's of $|\tilde{\psi}_1\rangle, \dots, |\tilde{\psi}_{k-1}\rangle$.

The i th iteration is described as follows:

1. Form the one-site right reduced density matrix $\rho_i, \tilde{\rho}_{1,i}, \dots, \tilde{\rho}_{k-1,i}$ from the orthogonality center $C_i, \tilde{C}_{1,i}, \dots, \tilde{C}_{k-1,i}$ at site i for $|\psi\rangle, |\tilde{\psi}_1\rangle, \dots, |\tilde{\psi}_{k-1}\rangle$ respectively.
2. Diagonalize ρ_i and get $\rho_i = V_i^\dagger S_i^2 V_i$. Not truncate here.
3. Form a projection operator onto the null space of C_i , i.e. $P_i = \mathbb{1} - V_i^\dagger V_i$.
4. If $P_i \neq 0$, do the summation $\tilde{\rho}_i = \tilde{\rho}_{1,i} + \dots + \tilde{\rho}_{k-1,i}$, and project $\tilde{\rho}_i$ by $\tilde{\rho}_i^\perp = P_i \tilde{\rho}_i P_i$.
5. Diagonalize $\tilde{\rho}_i^\perp$ and get $\tilde{\rho}_i^\perp = \tilde{V}_i^{\perp\dagger} \tilde{S}_i^{\perp 2} \tilde{V}_i^\perp$. Truncate η weights.
6. Enlarge the row space of V_i by direct sum with \tilde{V}_i^\perp and get $V_i' = [V_i \ \tilde{V}_i^\perp]^T$.

7. Multiply $V_i'^\dagger$ with $A_{i-1}C_i, \tilde{A}_{1,i-1}\tilde{C}_{1,i}, \dots, \tilde{A}_{k-1,i-1}\tilde{C}_{k-1,i}$ respectively and get the next orthogonality center $C_i, \tilde{C}_{1,i-1}, \dots, \tilde{C}_{k-1,i-1}$ at site $i - 1$.

Appendix F: Local subspace expansion

In the following we will take the left-to-right single-site TDVP sweep as an example to illustrate the local subspace expansion and the adjoint right-to-left sweep can be formulated similarly.

Just like the subspace expansion for the single-site DMRG, we use the expansion term with dimension $(m_{i-1}, d_i, w_i m_i)$

$$R_i = \alpha L_{i-1} W_i C_i. \quad (\text{F1})$$

where α is a constant to be tuned, L_{i-1} is the left edge tensor of the local effective Hamiltonian $H(i)$, and W_i is the tensor of the MPO of \hat{H} at site i .

The i th iteration is as follows:

1. Integrate the equation $i \frac{dC_i(t)}{dt} = H(i)C_i(t)$ and get $C_i(t + \Delta t)$.
2. SVD C_i and get $C_i = U_i S_i V_i$. Not truncate here.
3. Form a projector to the orthogonal complement of the column space of C_i , i.e. $P_i = \mathbb{1} - U_i U_i^\dagger$.
4. If $P_i \neq 0$, project $R_i = \alpha L_{i-1} W_i C_i$ by $R_i^\perp = P_i R_i$.
5. SVD R_i^\perp and get $R_i^\perp = U_i^\perp S_i^\perp V_i^\perp$. Truncate if necessary.
6. Enlarge the column space of U_i by direct sum with U_i^\perp , i.e. $U_i' = [U_i \ U_i^\perp]$.
7. Multiply $U_i'^\dagger$ with C_i and get $D_i = U_i'^\dagger C_i$.
8. Integrate the equation $-i \frac{dD_i(t)}{dt} = K(i)D_i(t)$ and get $D_i(t)$.
9. Multiply D_i with the next site tensor B_{i+1} and get the orthogonality center C_{i+1} at the next site.

Higher orders can be obtained by doing step 3 to 6 recursively.

ACKNOWLEDGMENTS

We thank Matthew Fishman, Alexander Wietek, Chia-Min Chong, Sean R. Muleady, Edwin M. Stoudenmire, and David J. Luitz for helpful discussions. The algorithms are implemented using the ITensor³² library. This work is funded by NSF through Grant DMR-1505406.

* mingrui@uci.edu

¹ S. R. White, Phys. Rev. Lett. **69**, 2863 (1992).

- ² S. R. White, Phys. Rev. B **48**, 10345 (1993).
- ³ E. Stoudenmire and S. R. White, Annual Review of Condensed Matter Physics **3**, 111 (2012).
- ⁴ S. R. White and A. E. Feiguin, Phys. Rev. Lett. **93**, 076401 (2004).
- ⁵ G. Vidal, Phys. Rev. Lett. **91**, 147902 (2003).
- ⁶ G. Vidal, Phys. Rev. Lett. **93**, 040502 (2004).
- ⁷ M. P. Zaletel, R. S. K. Mong, C. Karrasch, J. E. Moore, and F. Pollmann, Phys. Rev. B **91**, 165112 (2015).
- ⁸ J. Haegeman, C. Lubich, I. Oseledets, B. Vandereycken, and F. Verstraete, Phys. Rev. B **94**, 165116 (2016).
- ⁹ G. Vidal, Phys. Rev. Lett. **98**, 070201 (2007).
- ¹⁰ J. Haegeman, J. I. Cirac, T. J. Osborne, I. Pižorn, H. Verschelde, and F. Verstraete, Phys. Rev. Lett. **107**, 070601 (2011).
- ¹¹ M. Yang and S. R. White, Phys. Rev. A **99**, 022509 (2019).
- ¹² F. Verstraete, J. J. García-Ripoll, and J. I. Cirac, Phys. Rev. Lett. **93**, 207204 (2004).
- ¹³ C. D. White, M. Zaletel, R. S. K. Mong, and G. Refael, Phys. Rev. B **97**, 035127 (2018).
- ¹⁴ J. Haegeman, T. J. Osborne, and F. Verstraete, Phys. Rev. B **88**, 075133 (2013).
- ¹⁵ S. Goto and I. Danshita, Phys. Rev. B **99**, 054307 (2019).
- ¹⁶ S. R. White, Phys. Rev. Lett. **102**, 190601 (2009).
- ¹⁷ E. M. Stoudenmire and S. R. White, New Journal of Physics **12**, 055026 (2010).
- ¹⁸ U. Schollwöck, Annals of Physics **326**, 96 (2011).
- ¹⁹ E. Leviatan, F. Pollmann, J. H. Bardarson, D. A. Huse, and E. Altman, “Quantum thermalization dynamics with matrix-product states,” (2017), arXiv:1702.08894 [cond-mat.stat-mech].
- ²⁰ K. Hémerly, F. Pollmann, and D. J. Luitz, Phys. Rev. B **100**, 104303 (2019).
- ²¹ S. Paeckel, T. Khler, A. Swoboda, S. R. Manmana, U. Schollwöck, and C. Hubig, Annals of Physics **411**, 167998 (2019).
- ²² Y. Saad, SIAM Journal on Numerical Analysis **29**, 209 (1992).
- ²³ R. B. Sidje, ACM Trans. Math. Softw. **24**, 130 (1998).
- ²⁴ A. E. Feiguin and S. R. White, Phys. Rev. B **72**, 020404 (2005).
- ²⁵ The k required for the exact diagonalization will also be small, but its application to MPS suffers from problems such as the loss of orthogonality and production of highly entangled state.
- ²⁶ https://tensornetwork.org/mps/algorithms/denmat_mpo_mps/.
- ²⁷ C. Hubig, I. P. McCulloch, U. Schollwöck, and F. A. Wolf, Phys. Rev. B **91**, 155115 (2015).
- ²⁸ S. V. Dolgov and D. V. Savostyanov, SIAM Journal on Scientific Computing **36**, A2248 (2014).
- ²⁹ M. Kitagawa and M. Ueda, Phys. Rev. A **47**, 5138 (1993).
- ³⁰ J. Ma, X. Wang, C. Sun, and F. Nori, Physics Reports **509**, 89 (2011).
- ³¹ C. Hubig, J. Haegeman, and U. Schollwöck, Phys. Rev. B **97**, 045125 (2018).
- ³² ITensor Library (version 3.1.0) <http://itensor.org>.